BALLOONING MODE STABILITY FOR SELF-CONSISTENT PRESSURE AND CURRENT PROFILES AT THE H–MODE EDGE

R.L. MILLER, Y.R. LIN-LIU, T.H. OSBORNE, and T.S. TAYLOR

General Atomics, P.O. Box 85608, San Diego, California 92186-5608 USA

Presented at 39th Annual Meeting of DPP APS, Pittsburgh Nov. 19,1997

Work supported by the U.S. Department of Energy under Contract

DE-AC03-89ER51114.

GENERAL ATOMICS

Under what circumstances can self-consistent bootstrap current remove ideal ballooning limit on edge pressure gradient?

Sensitivity of "stiff" transport models to magnitude of edge pressure pedestal has recently increased the interest in maximum sustainable pressure gradient near tokamak plasma boundary

Equilibrium/infinite-n balloon stability calculations of pressure pedestal use TOQ and BALOO[1] to assess effects of elongation, triangularity, aspect ratio, pedestal location, pedestal width, q_{95}, and edge collisionality— ballooning calculations facilitated by improved numerics using approach of Bishop et al.[2]

Local pressure gradients near the boundary in DIII-D ELM-ing H-mode discharges exceed the first regime ballooning limit by up to factor of 2 [3]

Self-consistent bootstrap current typically raises the stability limit for the pressure gradient by reducing the local shear[4,5]

1. R.L. Miller, Y.R. Lin-Liu, A.D. Turnbull, V.S. Chan, L.D. Pearlstein, O. Sauter, and L. Villard, Physics of Plasmas **4** 1062 (1997).
2. C.M. Bishop, P. Kirby, J.W. Connor, R.J. Hastie, and J.B. Taylor, Nucl. Fusion **24** 1579 (1984).
3. T.H. Osborne, R.J. Groebner, L.L. lao, A.W. Leonard, R. Maingi, et al., EPS 1997.
4. Jackson, G.L., Winter, J. Taylor, T.S., Greenfield, C.M., Burrell, K.H. et al. Phys. Fluids B **4** 2181 (1992)
5. Deliyanakis, N., O'Brien, D.P., Balet, B. Greenfield, C.M., Perte L. et al., Plasma Phys. Control. Fusion **36** 1159 1994.

Specification of shape, pressure, and current profiles

Shape determined by aspect ratio (R_0/a), elongation (κ) and triangularity (δ):

$$R(\theta) = R_0 + a\cos\left(\theta + \sin^{-1}\delta\sin\theta\right)$$

$$Z(\theta) = \kappa a \sin\theta$$

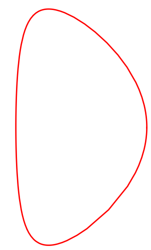

Note: No separatrix

Pressure profile has pedestal shape, width $\tilde{\psi}_{wid}$, and location of $p'_{max} = \tilde{\psi}_p$. p=0 at boundary.

$$p(\tilde{\psi}) = p_0\left(1 - \tanh\left[(\tilde{\psi} - \tilde{\psi}_p)/\tilde{\psi}_{wid}\right]\right)/2 -$$
$$p_0\left(1 - \tanh\left[(1 - \tilde{\psi}_p)/\tilde{\psi}_{wid}\right]\right)/2$$

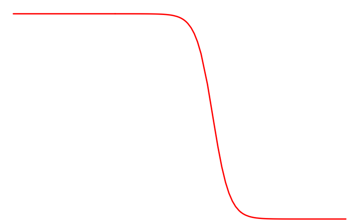

Plasma current is specified by

$$< J \cdot B >= JB_0\left(1 - \tilde{\psi}^{\mu}\right)^2$$

where JB_0 and μ are adjusted to determine q_{axis} and q_{95}. Bootstrap current is added to above formula. We use Hirshman[6] formulation for bootstrap which has the form

$$< J \cdot B >_{bs} = \mu_0 g(\psi) R B_T p'(\psi)$$

where $g(\psi)$ depends upon effective trapped particle fraction, Z_{eff}, and L_p/L_T the ratio of pressure to temperature scale lengths.

6. Hirshman, S.P., Phys. Fluids **31** 3150 (1988).

The reference equilibrium: κ=1.8, δ=0.3, A=170/65, $\tilde{\psi}_p$=0.98, $\tilde{\psi}_{wid}$=0.0125, q_{95}=3.5, and q_{axis}=1.1

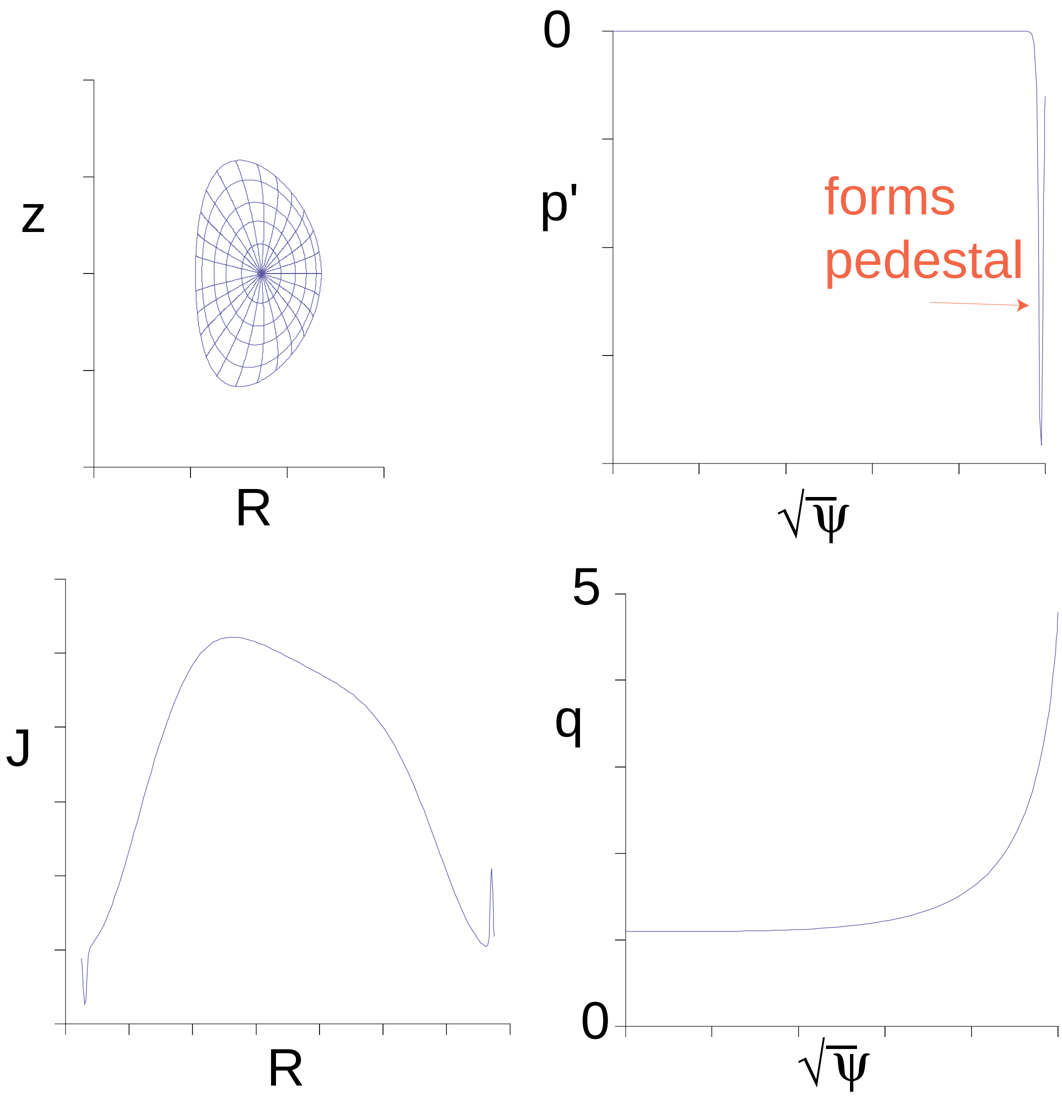

GENERAL ATOMICS

If bootstrap current is large enough, second stable access becomes possible

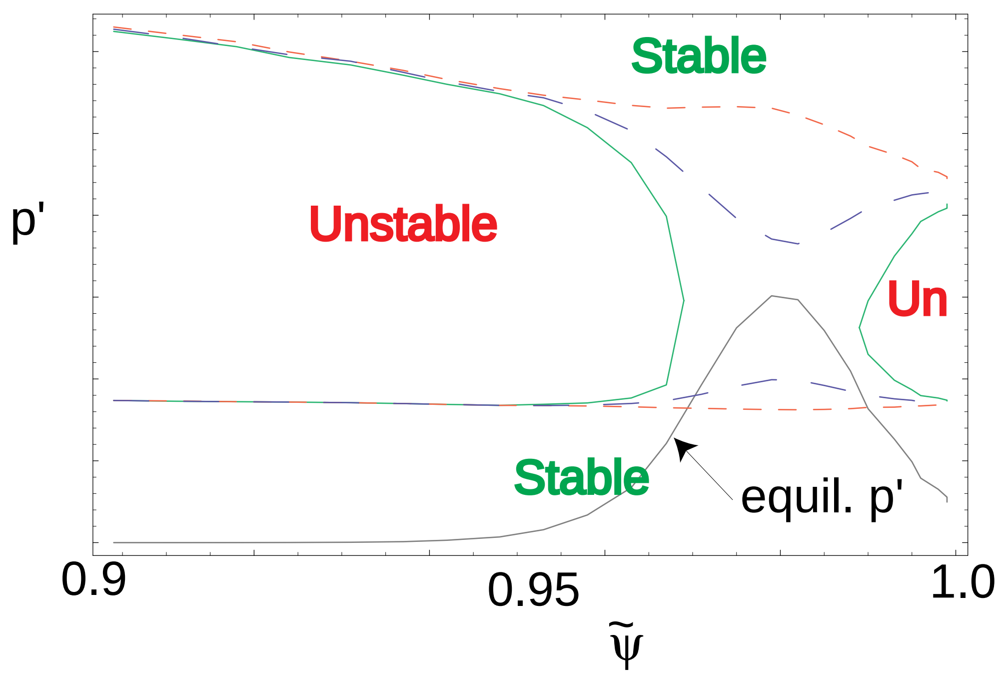

p' vs. $\tilde{\psi}$ along with first and second stability boundaries for Cboot = 0.0(short dash), 0.4(long dash) and 0.8(solid)

Strength of bootstrap current is artificially varied using Cboot

$$< J \cdot B >= JB_0\left(1 - \tilde{\psi}^{\mu}\right)^2 + C_{boot} < J \cdot B >_{bs}$$

Cboot=0 is no bootstrap
Cboot=1 is actual collisionless bootstrap

β/β_{NoBoot} vs C_{boot} for the reference equilibrium shows abrupt transition to second stable access

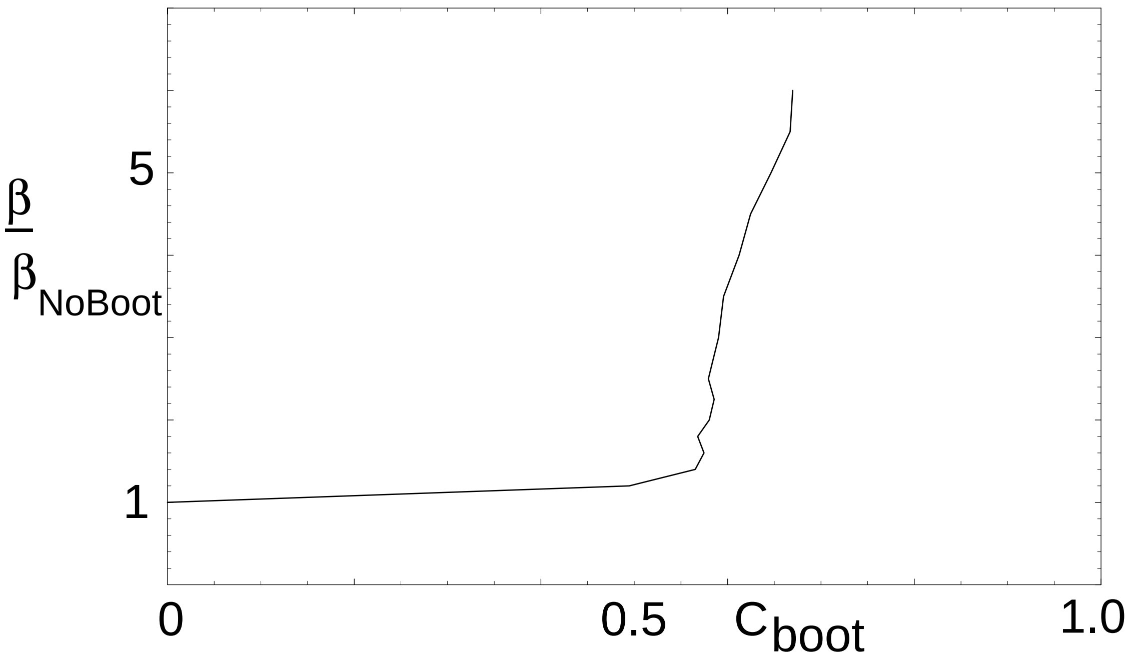

Transition to second stable access ~ C_{boot}=0.6

We define stable β/β_{NoBoot}=5 as second stable access. From here on, we report bootstrap current strength (C_{boot}) required to achieve β/β_{NoBoot}=5

GENERAL ATOMICS

C_{boot} vs. $\tilde{\psi}_p$ for $\tilde{\psi}_{wid}$=0.0125 shows second stable access more difficult for pedestal location at smaller radius $\tilde{\psi}_p$

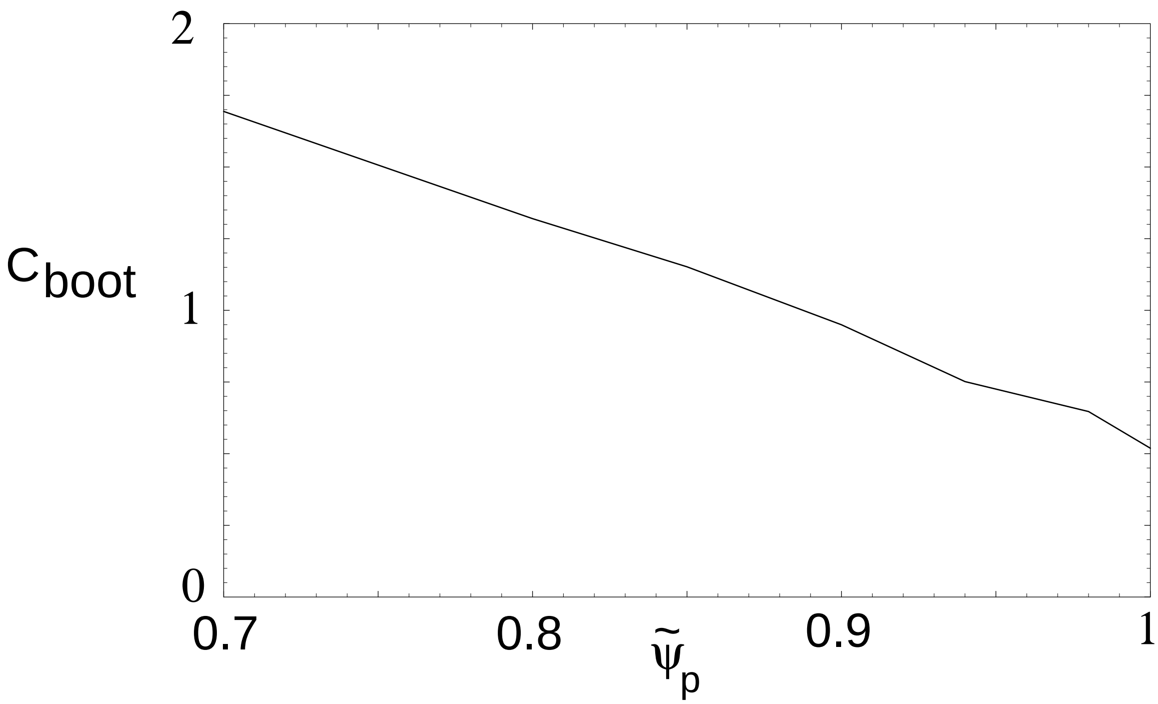

Note: $\tilde{\psi}_{wid}$= 0.0125 is consistent with DIII-D data.

GENERAL ATOMICS

C_{boot} vs. $\tilde{\psi}_{wid}$ for $\tilde{\psi}_p$=0.9 and $\tilde{\psi}_p$=0.98 shows second stable access more difficult for wider pedestal, $\tilde{\psi}_{wid}$ and smaller radius of pedestal location, $\tilde{\psi}_p$

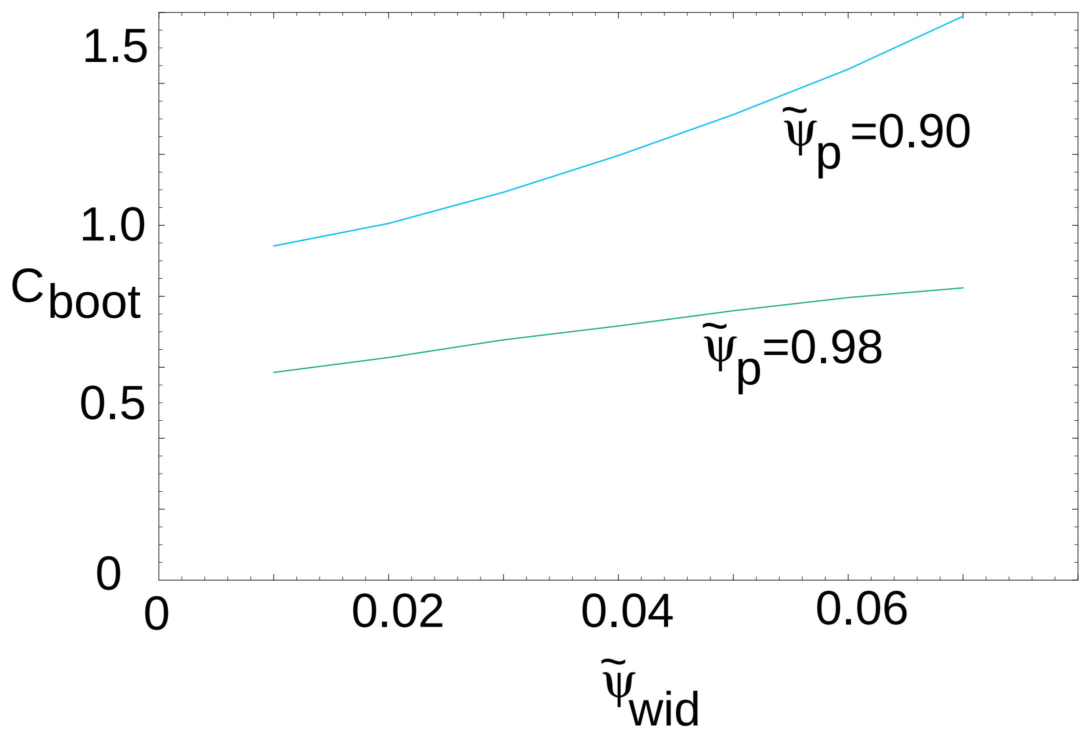

Cboot vs. δ for q_{95} = 2.5, 3.5, and 4.5 shows easier second stable access for higher q_{95} and intermediate δ

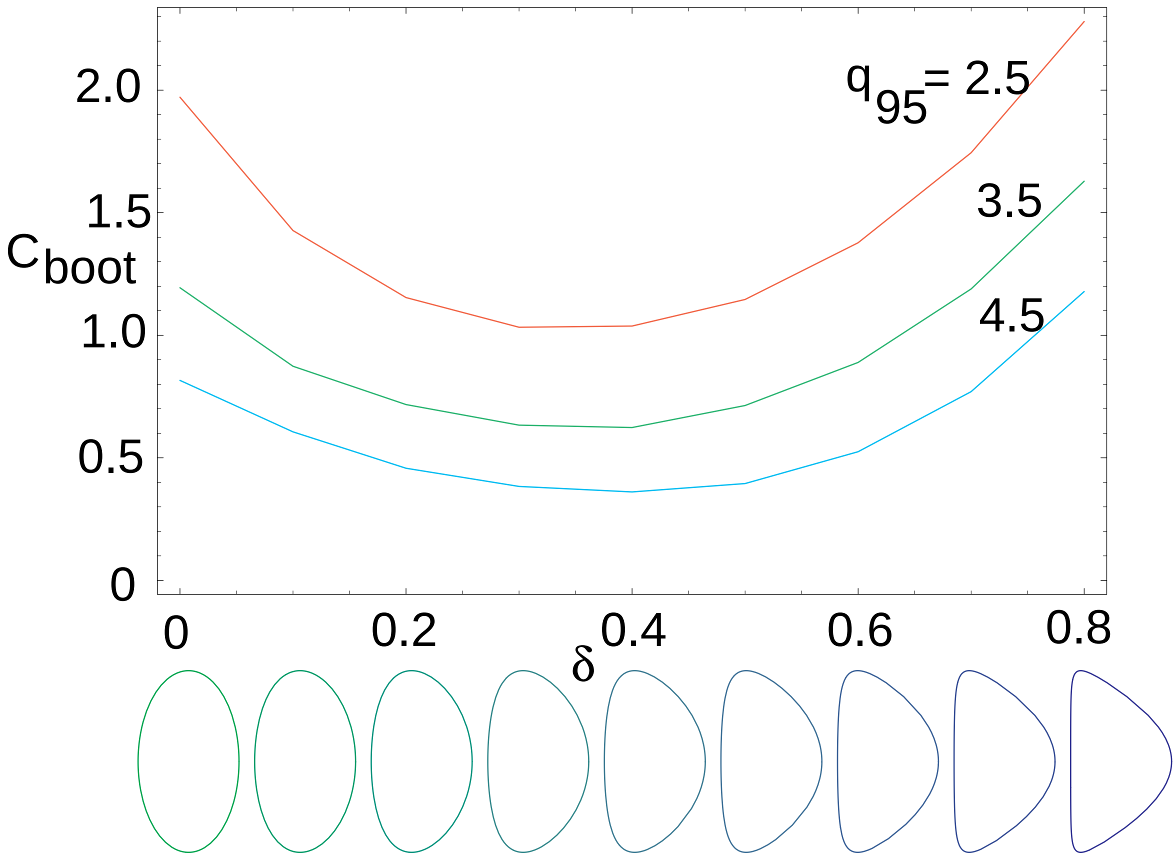

Raising q_{95} is seen to improve access to the second stable region as expected [7].

7. Lao L.L., Strait E.J., Taylor T.S., Chu M.S., Ozeki T., et al., Plasma Phys. & Cont. Fusion **31** 509 (1989).

Cboot vs. δ_2 shows a "blunter" dee has easier second stable access κ=1.8, δ=0.7

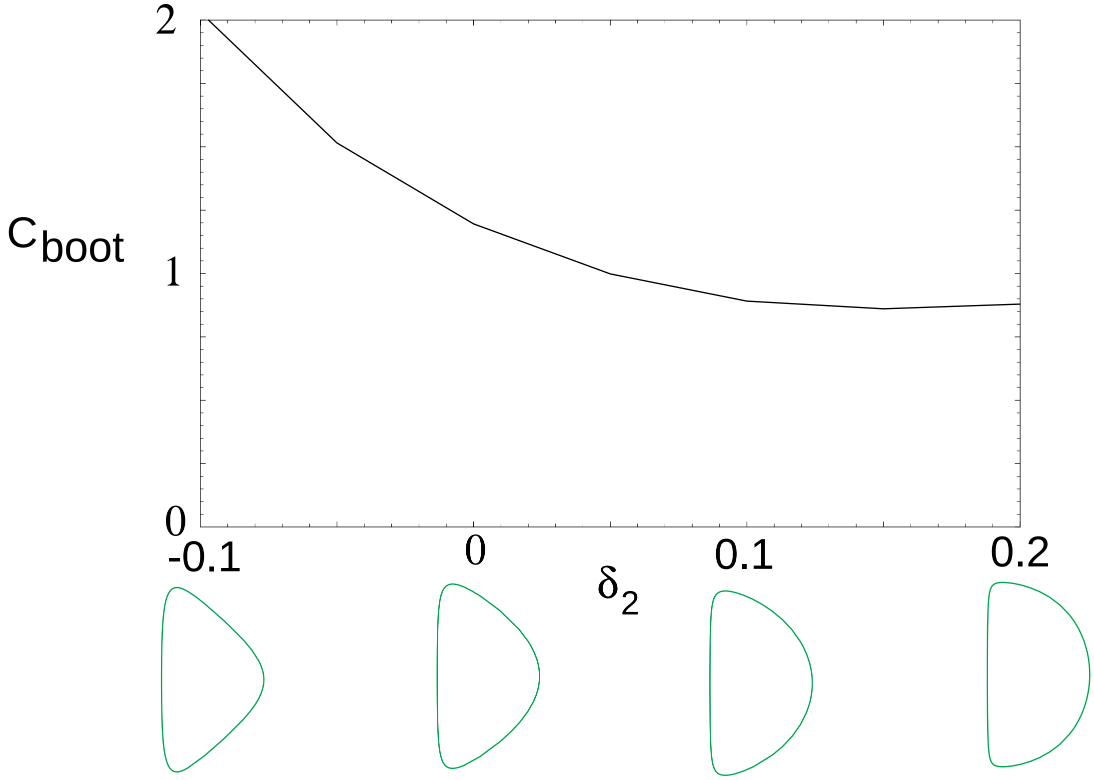

$$R(\theta) = R_0 + a\cos\left(\theta + \sin^{-1}\delta\sin\theta\right)$$

$$Z(\theta) = \kappa a\sin\left(\theta + \delta_2\sin 2\theta\right)$$

Bluntness or Squareness controlled by δ_2

GENERAL ATOMICS

Second stable access improves with larger κ

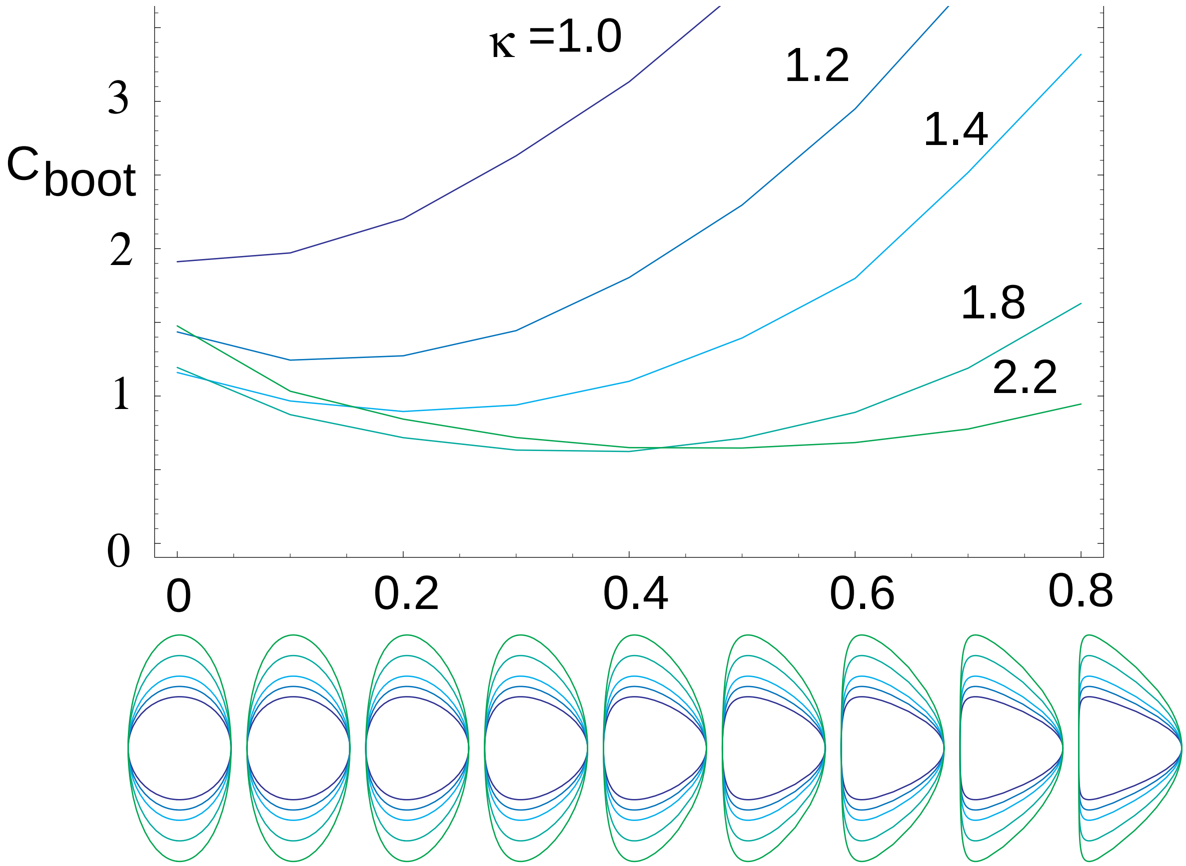

s-α diagram can help explain κ dependence

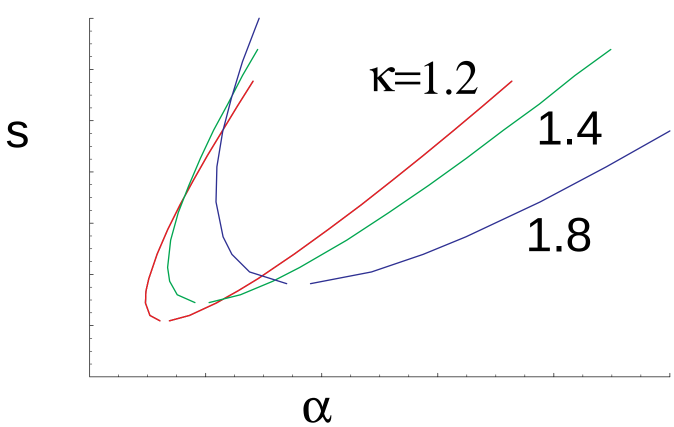

s-α "nose" higher for higher κ

first stable bndry higher for higher κ
-> more bootstrap
-> easier to reduce shear

Cboot vs. aspect ratio shows easier second stable access at large A

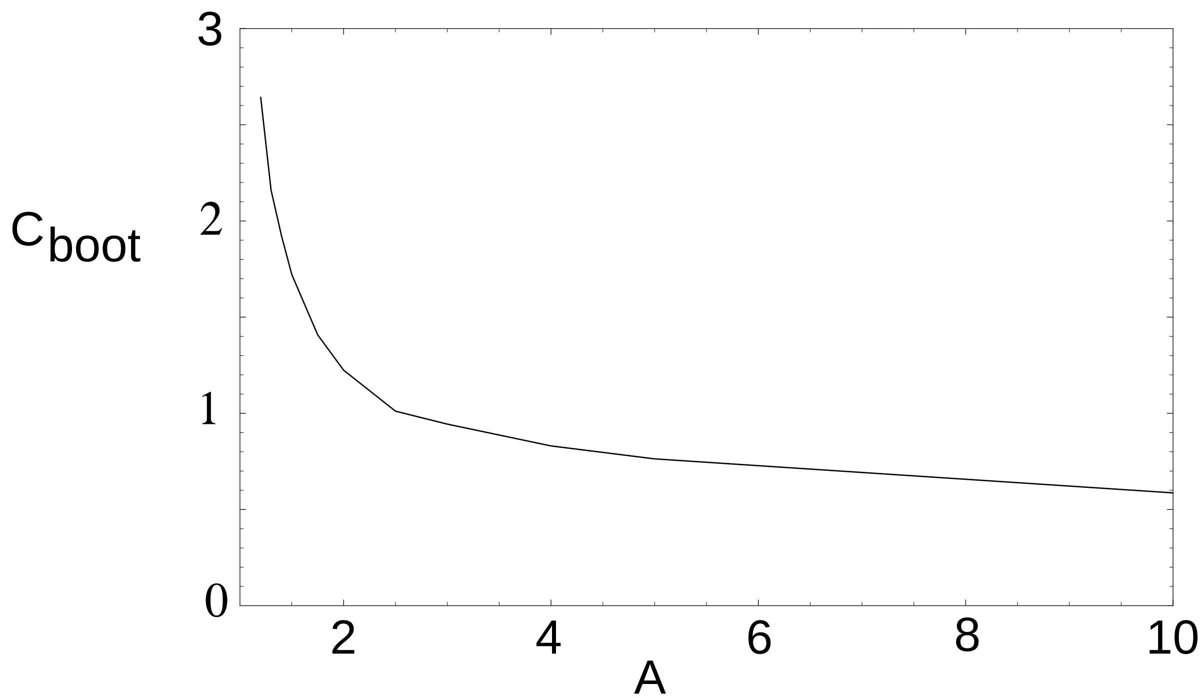

This scan is done at fixed μ

(recall $<J \cdot B> = JB_0\left(1-\tilde{\psi}^{\mu}\right)^2$) instead of fixed q_{95}.

As a result q_{95} is decreasing as A increases. At fixed q_{95}, the aspect ratio effect is even more pronounced.

One reason for aspect ratio effect is that bootstrap current fraction $\propto \beta_p/\sqrt{A}$

GENERAL ATOMICS

s-α diagrams help to interpret results

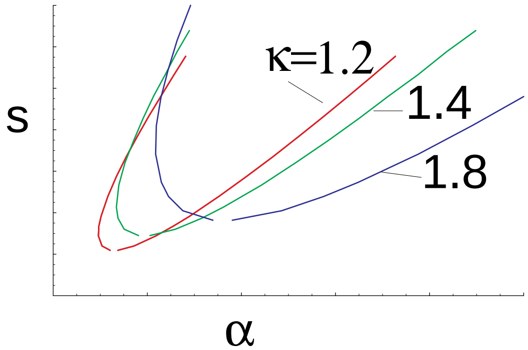

- **s-α nose rises with κ**
- **first stable bndry allows more bootstrap at higher κ**

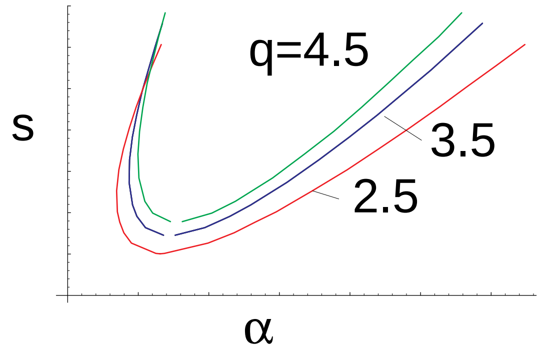

- **s-α nose rises with q**
- **first stable bndry allows more bootstrap at higher q**

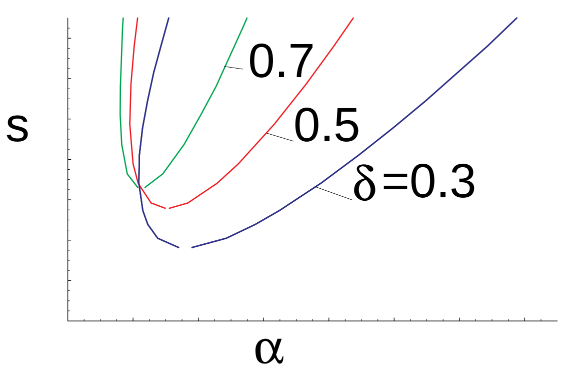

- **s-α nose rises with δ**
- **first stable bndry allows more bootstrap at lower δ**
- **also larger trapped particle fraction at lower δ -> higher bootstrap**

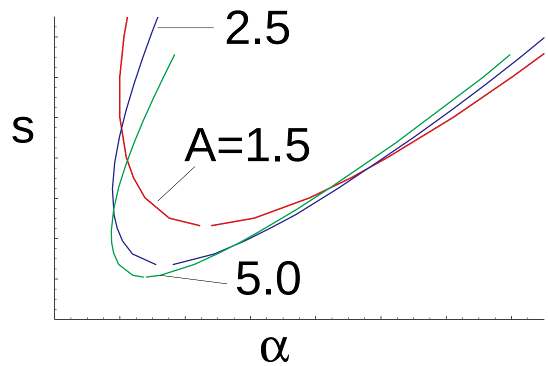

- **s-α nose lowered with A but so is s_{equil}**
- **first stable bndry implies more bootstrap at lower A but $A^{-1/2}$ scaling defeats it.**

Collisional effects reduce bootstrap current and make second stable access more difficult

$n_{edge} = 2\text{x}10^{19} m^{-3}$

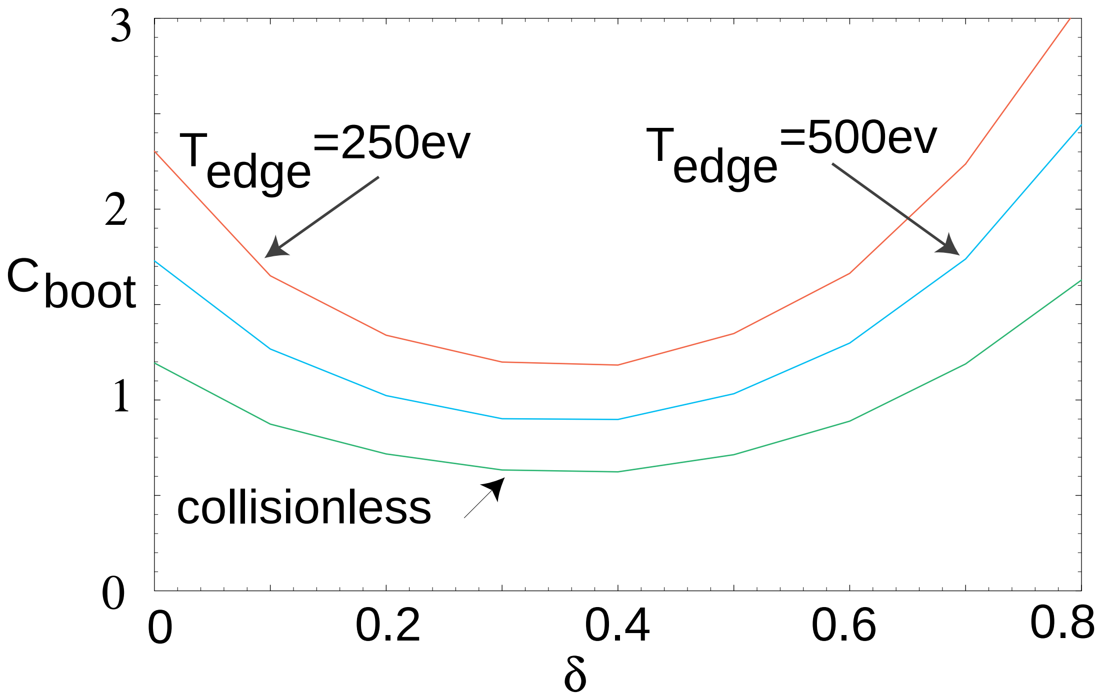

Used collisional model of Sauter et al. [8] to compare with collisionless Hirshman[6]. Collisional effects can be roughly approximated by $J_{boot} \to J_{boot}/\left(1+\sqrt{\nu_*}\right)$

Ranges of average values for H-mode plasmas in DIII-D are $n_{edge} = 1-6\text{x}10^{19} m^{-3}$ and $T_{edge} = 50-300 ev$[9].

8. Sauter O., Lin-Liu Y.R., Hinton F.L., and Vaclavik J., Theory of Fusion Plasmas (Proc. Joint Varenna-Laussane Int. Workshop, Varenna, 1994), Editrice Compositori, Bologna.
9. Gary Porter, private communication.

GENERAL ATOMICS

Density gradient is more effective than temperature gradient for achieving second stable access—effect is more pronounced when collisional

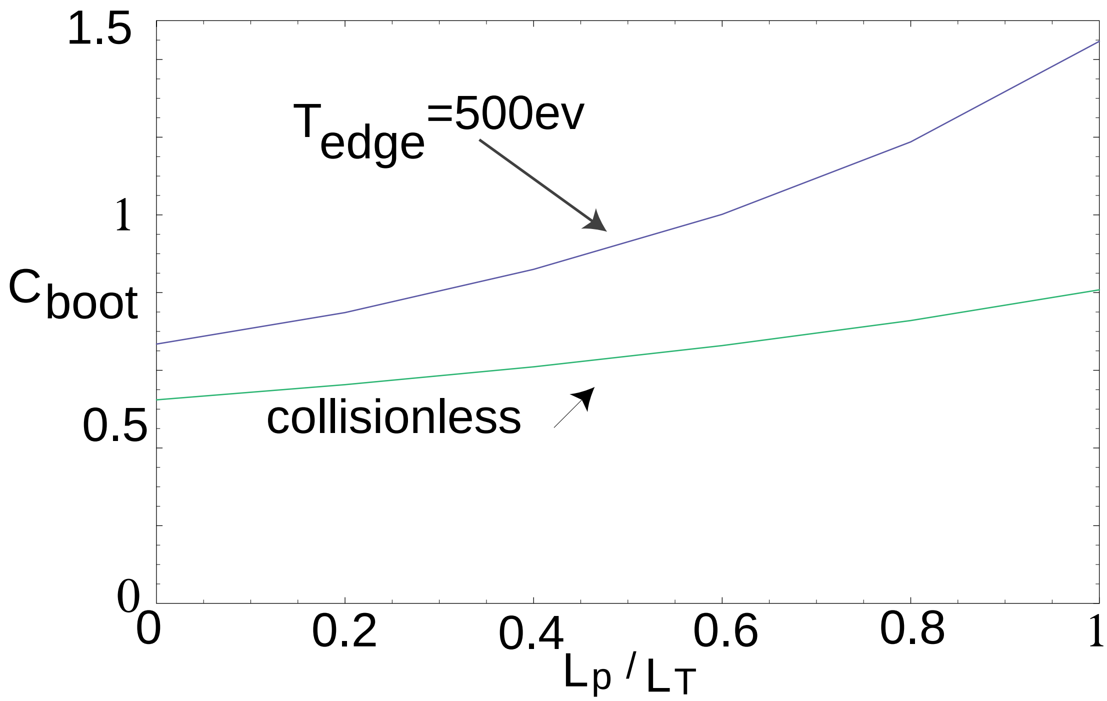

$n_{edge} = 2x10^{19} m^{-3}$

Summary

Transition to second stability is easier for:

- **higher elongation κ**
- **intermediate triangularity δ**
- **larger aspect ratio A**
- **larger pedestal formation radius $\tilde{\psi}_p$**
- **narrower barrier width $\tilde{\psi}_{wid}$**
- **higher q_{95}**
- **lower collisionality ν_***

A more complete ideal MHD picture of self-consistent bootstrap current at the edge should include stability to low-n modes as well. [10-11]

10. E.J. Strait, T.S. Taylor, A.D. Turnbull, M.S. Chu, J.R. Ferron, L.L. Lao, and T.H. Osborne, EPS I-211 1993.
11. Huysmans, G.T.A., Challis, C.D., Erba, M., Kerner, W. and Parail, V.V., EPS I-201 1995.